AGU PUBLICATIONS

Geophysical Research Letters

RESEARCH LETTER
10.1002/2016GL068269

Key Points:
- Many MJOs have gradual shallow-to-deep transitions consistent with convective moistening time scale
- Rapid transitions (one week) with convective outbreak are not rare (25% of the time)
- Time scale of shallow-to-deep transition is negatively correlated with duration of suppressed period

Correspondence to:
W. Xu,
wxinxu@atmos.colostate.edu

Citation:
Xu, W., and S. A. Rutledge (2016), Time scales of shallow-to-deep convective transition associated with the onset of Madden-Julian Oscillations, *Geophys. Res. Lett.*, *43*, 2880–2888, doi:10.1002/2016GL068269.

Received 14 FEB 2016
Accepted 1 MAR 2016
Accepted article online 6 MAR 2016
Published online 16 MAR 2016

Time scales of shallow-to-deep convective transition associated with the onset of Madden-Julian Oscillations

Weixin Xu[1] and Steven A. Rutledge[1]

[1]Department of Atmospheric Sciences, Colorado State University, Fort Collins, Colorado, USA

Abstract This study statistically investigates the timing and underlying processes of the shallow-to-deep convective transition (SDT) associated with Madden-Julian Oscillations (MJO) initiation over the Indian Ocean. Results show that SDT periods have a median value of 8–10 days with a wide spectrum of 2–20 days. SDTs lasting 10–20 days occurred nearly 50% of the time, consistent with gradual tropospheric moistening and destabilization leading to MJO initiation as described by the discharge-recharge theory. Rapid SDTs (<7 days) took place in 25% of the MJOs studied, including two MJOs observed during Dynamics of the MJO in which previous studies suggested large-scale moistening dominates the local convective moistening during SDT. SDT length is only weakly correlated to MJO amplitude and duration defined by the Real-Time Multivariate MJO index. SDT length is negatively correlated with the duration of the shallow convective period preceding the SDT but weakly correlated with individual parameters associated with preonset environments.

1. Introduction

The Madden-Julian Oscillation (MJO) is the most dominant mode of intraseasonal variability in the tropics [*Madden and Julian*, 1971, 1972; *Zhang*, 2005], having broad impacts on global weather and climate (summary in *Zhang* [2013]). However, the MJO has been poorly simulated by several generations of general circulation models [*Lin et al.*, 2006; *Hung et al.*, 2013], especially the convective initiation phase over the equatorial Indian Ocean (IO) [*Bechtold et al.*, 2008; *Kim et al.*, 2009; *Vitart and Molteni*, 2010].

Initiation of the MJO active phase is usually indicated by the transition from a mode of shallow, isolated convection to a widespread, deep convective mode. One of the popular mechanisms responsible for this initiation process is the so-called "discharge-recharge" theory [*Bladé and Hartmann*, 1993; *Hu and Randall*, 1994; *Kemball-Cook and Weare*, 2001; *Benedict and Randall*, 2007]. This theory proposes a positive feedback between the depth of cumulus convection and tropospheric humidity (starting from moistening by shallow convection) until the large-scale environment is sufficiently moist to support copious amounts of deep convection. It is proposed that this moistening and deepening process by cumulus and congestus typically occurs over a 10–15 day period [*Kemball-Cook and Weare*, 2001; *Benedict and Randall*, 2007]. Many observational studies support the importance of cloud moistening during MJO initiation [*Stephens et al.*, 2004; *Benedict and Randall*, 2007; *Riley et al.*, 2011; *Del Genio et al.*, 2012]. Indeed moistening and heating of the lower troposphere by shallow convection is a key factor for successful simulations of the MJO in climate models [*Zhang and Song*, 2009; *Del Genio et al.*, 2012].

However, the time scale of the moistening by cumulus and congestus during the shallow-to-deep transition (SDT) as formulated by the discharge-recharge mechanism has been questioned recently. New observational studies [*Powell and Houze*, 2013, 2015a; *Ruppert and Johnson*, 2015] showed that the SDT (or building period) during the onset of two MJOs over the central IO occurred over a 3–7 day period as observed by island-based radar, spaceborne radar, and rawinsonde observations during the Dynamics of the MJO field campaign (DYNAMO) [*Yoneyama et al.*, 2013]. A similar SDT time period (4–6 days) would be inferred from DYNAMO shipborne radar data [*Xu and Rutledge*, 2014; *Xu et al.*, 2015], if a similar SDT definition as in *Powell and Houze* [2015a] is applied. *Powell and Houze* [2015a, 2015b] argued that different mechanisms other than the discharge-recharge mechanism must be responsible for MJO initiation because SDT time periods during the DYNAMO events (3–7 days) were significantly shorter than the 10–20 days proposed by the discharge-recharge theory. They further proposed that the reduction in large-scale subsidence associated with an eastward propagating feature played an important role in helping the troposphere moisten rapidly, thus shortening the SDT

time period [*Powell and Houze*, 2015b]. Similarly, *Ruppert and Johnson* [2015] found that the reduction of large-scale subsidence coincided with the moisture increase in the lower-to-middle troposphere, suggesting its potential role in tropospheric moistening. Furthermore, high-resolution model simulations demonstrated that the moisture buildup leading to the initiation of MJOs during DYNAMO was mainly caused by large-scale uplift along with the decline of large-scale drying by equatorward advection [*Hagos et al.*, 2014]. Simulations by *Hagos et al.* [2014] further indicated that convective-scale moisture variability and uplift only played secondary roles. Their findings are similar to studies regarding SDT of general tropical convective systems not related to MJO [*Hohenegger and Stevens*, 2013; *Masunaga*, 2013].

In short, studies based on composites of multiple MJOs using reanalysis or satellite data support the discharge-recharge mechanism [*Benedict and Randall*, 2007; *Riley et al.*, 2011; *Del Genio et al.*, 2012], while DYNAMO case studies suggest that large-scale moistening dominated more local convective moistening (discharge-recharge) during SDT periods. However, neither climatological composites nor DYNAMO-based studies addressed the full spectrum of SDTs; thus, SDT time scales and associated processes are still open to question. Indeed *Powell and Houze* [2015a] stated that longer SDT periods, consistent with the discharge-recharge mechanism could apply to other MJO cases, as their study was limited to the two DYNAMO-specific cases. So the central question we address in this study is the following: what is the distribution of the SDT period over a large sample of MJOs? Related questions we address include, what is the relationship between SDT and the particular MJO strength/duration? Do MJOs with rapid SDT have stronger convection (or heavier precipitation) than those with gradual SDT or vice versa? Are their environmental characteristics distinctly different when SDT is short compared to when SDT is long?

2. Data and Methodology

Using Tropical Rainfall Measuring Mission (TRMM) data and additional data resources, this study examines the convective evolution (mainly SDT) and associated environmental conditions of MJOs during 1998–2013 over an extended region (68–88°E, 8°S–8°N) centered on the location of the DYNAMO [*Yoneyama et al.*, 2013] sounding arrays (Figure 1a). This region is particularly selected as it has DYNAMO observations to guide analysis and sufficient TRMM satellite sampling.

2.1. Data Resources

The version 7 TRMM Multisatellite Precipitation Analysis (3B42) rainfall product [*Huffman et al.*, 2007] provides continuous (3-hourly) rainfall time series over the study region. For the DYNAMO-specific MJOs, high-resolution (2 km, hourly) gridded radar data (in 150 km range) collected from the R/V *Roger Revelle* C band radar (located at 80.5 E, 0 N) are used to estimate radar echo top heights as proxies of convective depth [*Xu et al.*, 2015]. The evolution of cloud tops during DYNAMO are based on infrared (channel 8) measurements from Meteosat-7 (spatial resolution of 5 km and a frequency of 30 min), provided by the European Organization for the Exploitation of Meteorological Satellites. Sea surface temperature (SST) evolution for MJOs during 1998–2013 is derived from the TRMM Microwave Imager and Advanced Microwave Scanning Radiometer for EOS [*Gentemann et al.*, 2010]. The European Centre for Medium-Range Weather Forecasts Re-Analysis Interim reanalysis data [*Dee et al.*, 2011] were used to calculate lower tropospheric (10 m) winds and midtropospheric (500 hPa) relative humidity.

2.2. Selection of MJO Events Initiated Over the IO

MJO cycles are identified using the Real-Time Multivariate MJO (RMM) index [*Wheeler and Hendon*, 2004] (hereafter WH index). WH index assigns eight different phases globally. Over the IO, the suppressed, building, active, and post-MJO conditions are usually marked by phases 6-7, 8-1, 2-3, and 4-5, respectively. Since this study focuses on the evolution of the MJO from suppressed conditions to the onset of the deep convection over the IO, we select MJO events from the climatology that encompass at least the suppressed, building, and active phases consecutively (phase 6, 7, 8, 1, 2, 3) defined by the WH index. A significant MJO is defined here as having a daily rainfall amount (averaged over the study region) greater than 5 mm d^{-1}. After applying these definitions, 94 full MJO cycles were identified during 1998–2013. These MJO events underwent further scrutiny using a TRMM sampling test (section 2.3). As a result, final set of 74 MJOs passing all the criteria was selected, including the two MJO events (November and October 2011) during DYNAMO.

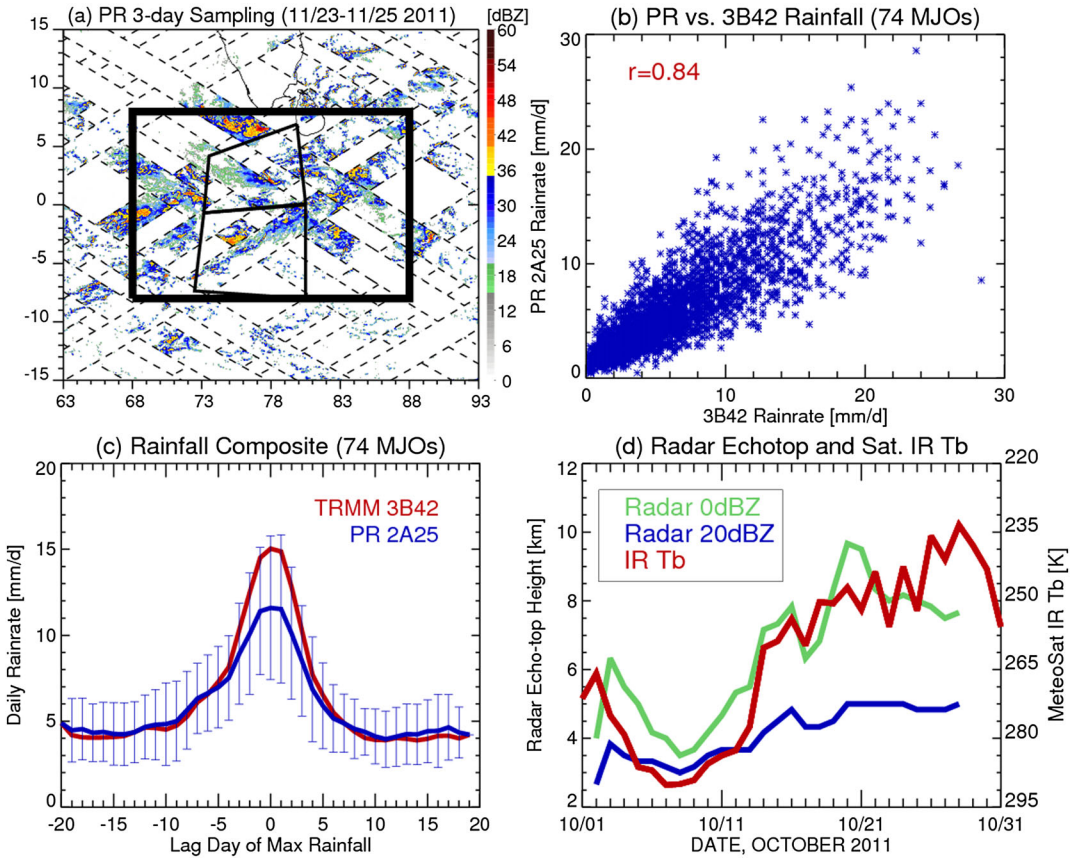

Figure 1. (a) TRMM PR swath and near surface radar reflectivity during a three day period (23 November–25 November 2011) over the study region (black rectangle) and the DYNAMO arrays (quadrilateral boxes), (b) scatter views on PR 2A25 versus 3B42 daily rainfall averaged over the study region (*r* is the correlation coefficient), (c) daily rainfall composite of the selected 74 MJO events (error bars represent the standard deviation of difference between 2A25 and 3B42), and (d) time series of median radar echo top heights and satellite IR T_b over the DYNAMO Revelle radar domain during the 2011 October MJO. Note that a 3 day running mean filter has been applied to the PR and 3B42 daily rainfall time series.

2.3. Using TRMM Observations to Define SDT

Sixteen years of TRMM level 1 data from the Precipitation Radar (PR) and the Visible/Infrared Sensor (VIRS) [*Kummerow et al*., 1998] are used to examine the convective evolution of MJO cycles over the defined region (Figure 1a). There are a significant number of TRMM overpasses (total of ~11,000) across the MJO life cycle. TRMM overpassed the region 3–4 times daily with a PR coverage area of ~30% (Figure 1a). A 3 day running mean filter is applied to the daily data to increase TRMM's sampling of a daily data point. In order to evaluate the capability of TRMM satellite imagery to resolve MJO convective evolution, PR rainfall estimates are compared to the 3B42 rainfall data with higher time resolution (3-hourly). Approximately 80% of MJOs (74 out of 94) were deemed to be well sampled by TRMM (i.e., to have well-matched rainfall evolution patterns between PR and 3B42). Both scatterplots (Figure 1b) and composites (Figure 1c) of daily rainfall (regional mean) during the selected 74 MJOs show good consistency between PR and 3B42. Therefore, we argue that TRMM sampling is able to resolve the MJO convective evolution (daily regional mean).

By definition, SDT is the transition from a shallow cumulus (e.g., cloud top $<$ 4–5 km) mode to the deep convective mode (e.g., cloud top $>$ 9–10 km) [*Johnson et al*., 1999]. Previous DYNAMO studies regarding the SDT are based on 20 dBZ echo top heights from ground-based radar [*Powell and Houze*, 2013; *Hagos et al*., 2014] and TRMM PR [*Powell and Houze*, 2015a]. However, the 20 dBZ echo top height has small changing dynamics (3–5 km) (also in *Powell and Houze* [2015a]) and maximizes only near the freezing level (~5 km), which is not so indicative of deep convection according to *Johnson et al*. [1999], so this

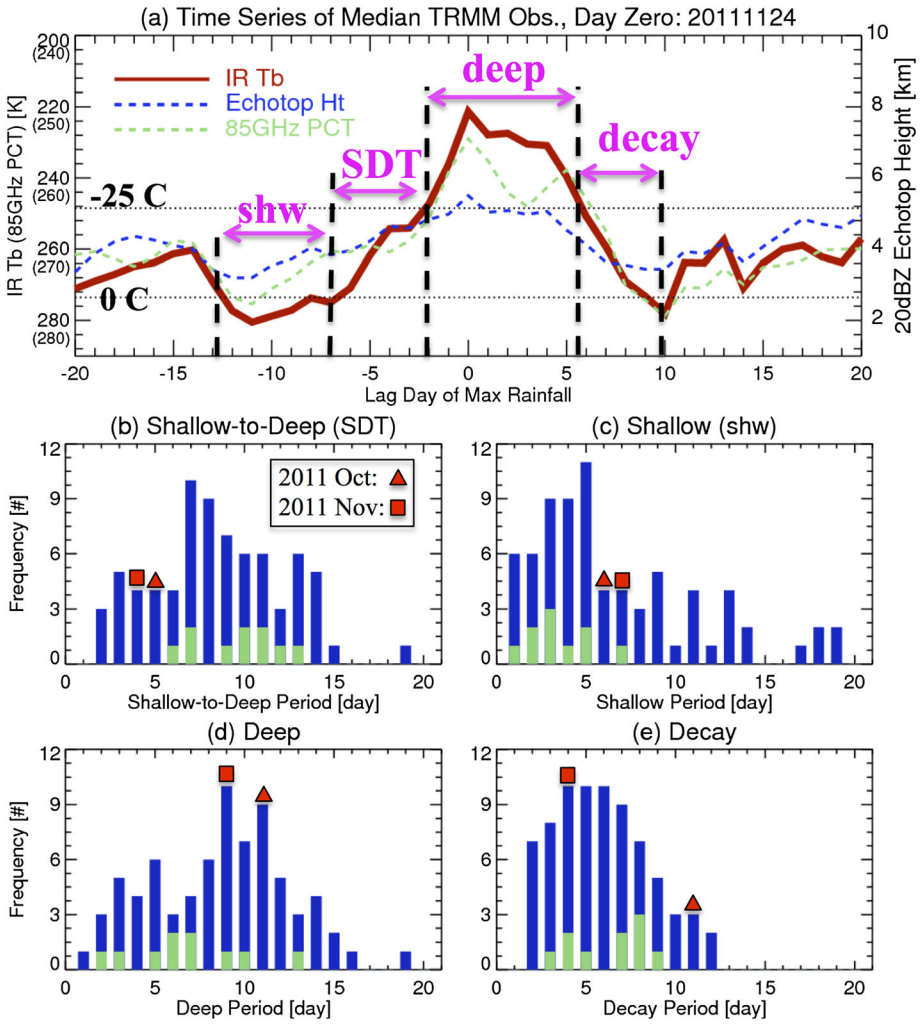

Figure 2. (a) Time series of median values of TRMM VIRS IR T_b (red solid line) during the 2011 November MJO event as an example for defining shallow convection (shw), shallow-to-deep transition (SDT), deep convection (deep), and decaying (decay) periods. (b–e) The frequency of MJO events (total of 74) as a function of length of different convective periods: (b) SDT, (c) shallow convection, (d) deep convection, and (e) decaying. Note that green bars indicate primary MJOs during 1998–2010. DYNAMO MJOs during October and November 2011 are marked in red triangle and square, respectively.

metric may not be the best metric for identifying SDT. In contrast, the 0 dBZ echo top height and IR T_b peaks 4–5 km higher than the 20 dBZ echo top and clearly depicts a substantial increasing trend (3–10 km) in echo top height associated with SDT. Since the lowest detectable echoes for the PR is 17–18 dBZ, this study uses VIRS IR T_b to define SDT trends of MJO convection. In order to include only convective clouds and remove cirrus contamination, IR T_b is constrained to the convective rain area defined by TRMM PR. Note that cirrus frequently occurs 30° east of the main MJO convection [*Virts and Wallace*, 2010].

IR T_b from VIRS is first interpolated onto the convective areas of the PR swath as defined by the TRMM 2A25 algorithm [*Awaka et al.*, 2009]. Time series of these "convective IR T_b" values are then employed to define various convective periods of the MJO (red curve in Figure 2a). Similar definitions as *Kikuchi and Takayabu* [2004] are applied: shallow convection is defined as IR $T_b < 0$°C (or 5 km asl), SDT as -25°C < IR $T_b < 0$°C, deep convection as IR $T_b < -25$°C (or 9 km asl), and the decaying period as -25°C < IR $T_b < 0$°C (Figure 2a). The SDT is considered when there is an increasing trend starting from the freezing level. Prior to the SDT, minor fluctuations (e.g., <5°C) around the freezing level are still considered to be associated with the shallow convective period. Per this definition, the two DYNAMO MJOs had SDT time scales of 4–5 days (Figure 2b), very similar to the 3–7 day time scales based on DYNAMO radar data [*Powell and Houze*, 2013].

3. Results

3.1. Time Scales of SDT and Other Convective Periods

The 74 MJOs available for investigation during 1998–2013 range from weak to strong (RMM amplitude = 0.5–2.5), less rainy to heavily precipitating (maximum rain rates of 5–35 mm d^{-1}), and short to long-lasting events (RMM duration = 20–80 days). The life cycle of these MJOs (20–80 day) is consistent with MJO's climatological variability [*Lafleur et al*., 2015]. Therefore, this study is not biased to a particular type of MJO event but captures the broad variability documented by many previous studies. The two MJOs sampled during DYNAMO had large RMM amplitudes (2.0–2.5) and produced large amounts of rainfall (25–30 mm d^{-1}), yet their durations (30–40 days) were about average based on our climatology. Statistics show that MJO amplitude and duration are only weakly correlated to the time scale and convective intensity of various MJO periods such as the SDT ($r = 0.25$–0.3). In other words, RMM-based MJO duration does not indicate the length of SDT nor does RMM amplitude correspond well to the intensity of MJO deep convection.

SDT time scale (Figure 2b) exhibits a broad spectrum from 2 days to more than 2 weeks with the median values around 8–10 days (Figure 2b). Nearly 50% of the SDT spectrum is situated in the 10–20 day time scale, consistent with the gradual buildup of atmospheric instability through low-level warming/moistening and radiative cooling aloft as proposed in the discharge-recharge theory [*Benedict and Randall*, 2007]. Discharge-recharge theory posits that shallow cumulus and congestus gradually warm and moisten the lower-free troposphere leading to widespread destabilization. On the other hand, rapid SDT (less than 1 week) occurs in ~25% of the MJOs sampled by TRMM. SDT periods for the two DYNAMO MJOs defined by our IR-based method are at the lower end of the SDT spectrum at 4–5 days (marked in Figure 2b), consistent with the SDT periods reported by the previously cited DYNAMO studies [*Powell and Houze*, 2013; *Ruppert and Johnson*, 2015; *Powell and Houze*, 2015a]. These studies suggest that moistening in the SDT periods by large-scale mechanisms (e.g., uplift) dominates the local convective moistening [*Hagos et al*., 2014; b]. As mentioned previously, the correlation between SDT period and both the magnitude (RMM index) and duration of individual MJOs is weak ($r < 0.3$). In other words, rapid (gradual) SDT is not statistically associated with short (long) duration MJOs. Also, there is no evidence that strong (weak) MJOs (by RMM index) tend to have rapid (gradual) SDT. In addition, SDT does not influence the convective depth or precipitation intensity of MJO deep convection ($r < 0.2$).

The shallow convective period (SCP) prior to SDT has a median value of 5–6 days (Figure 2c), a few days shorter than the SDT. Some extended SCPs lasting more than 2 weeks were also present in our data set. The length of the deep convective period after SDT is usually 9–11 days but ranges from 1 to 20 days (Figure 2d). In terms of the duration of the shallow and deep convective periods, the two DYNAMO MJOs are near the climatological mean. SCP duration is only weakly correlated to MJO duration or magnitude ($r = 0.25$), whereas the duration of the deep convective phase is slightly correlated to the MJO magnitude as defined by the RMM index ($r = 0.3$–0.35). The duration of the deep convective period, however, is well correlated with convective intensity as indicated by the coldest clod top ($r = 0.62$). Finally, the decaying convective period exhibits a mode of shorter time scales (5–6 days) and less variability (Figure 2e) compared to the SDT, suggesting convective dissipation and tropospheric drying occur more rapidly than cumulus growth and tropospheric moistening [*Benedict and Randall*, 2007].

3.2. Relationships Among SDT, SCP, and Environmental Factors

Figure 3 shows statistical relationships between time scales of different convective periods (e.g., SDT versus SCP) and environmental factors (only parameter pairs with significant correlations are shown). It is interesting that SDT time scale is (significantly) negatively correlated to SCP duration (Figure 3a), that is, longer SCP implies shorter SDT and vice versa. Both SDT and SCP durations are weakly correlated ($r = 0.2$–0.3) with a single parameter of preonset environments (e.g., SST, winds, and midtropospheric humidity), possibly due to the fact that they are influenced simultaneously by multiple environmental factors/processes. The exception is that SCP duration correlates (significantly) negatively with midtropospheric (500 hPa) relative humidity (RH, Figure 3b), which is reasonable, as a dry midtroposphere (also indicative of large-scale descent) could suppress the growth of congestus due to strong dry air entrainment (or large-scale descent) until sufficiently moist conditions are reached. SST during SDT significantly affects the intensity of the following deep convective period (Figure 3c), possibly by providing high surface heat fluxes and greater instability to the atmosphere [*Xu and Rutledge*, 2014]. The low-level winds influence the atmospheric convection by modifying the wind shear and surface heat fluxes, for instance SST is negatively correlated to the lower tropospheric winds (Figure 3d) associated with latent

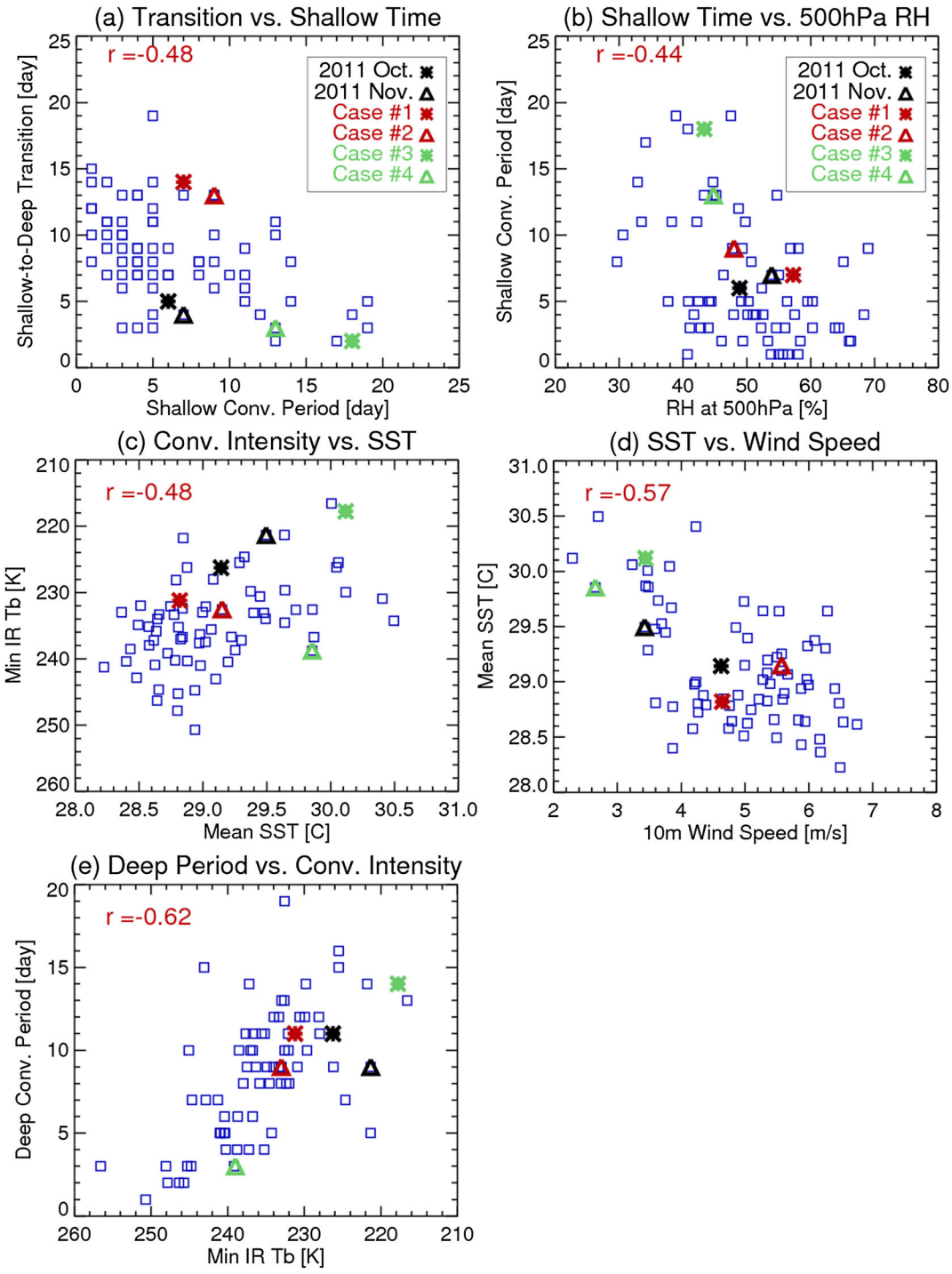

Figure 3. Scatter distribution of MJO events (total of 74) as a function of: (a) length of shallow-to-deep transition versus shallow convection period, (b) duration of shallow convective period versus relative humidity (RH) at 500 hPa, (c) convective intensity versus SST, (d) SST versus wind speed at 10 m, and (e) duration of deep convective period versus Min IR T_b. RH, SST, and winds are considered prior to the onset of MJO deep convection. Correlation coefficients (r) are marked in the red text. The two DYNAMO MJOs and four selected MJO cases are also marked.

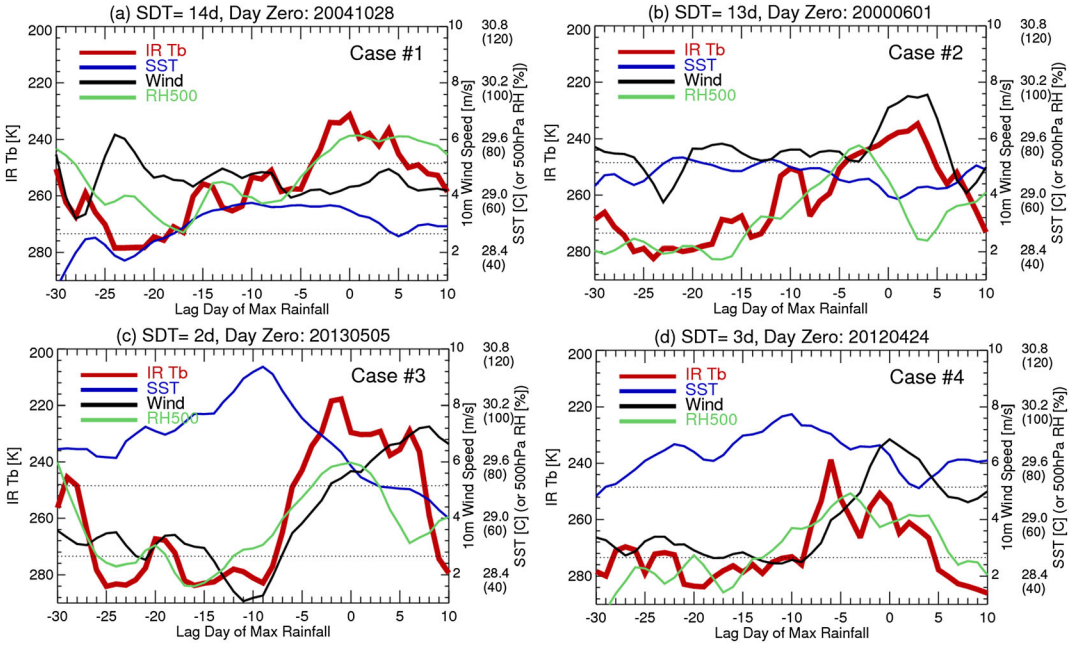

Figure 4. Time series of four MJO cases (as marked in Figure 3) in periods of: (a) 28 September–7 November 2004, (b) 2 May–11 June 2000, (c) 5 April–15 May 2013, and (d) 23 March–4 May 2012. Parameters include convective cloud top brightness temperature (IR T_b), sea surface temperature (SST), 10 m wind speed (wind), and relative humidity at 500 hPa (RH500). Time series is presented as a function of lag day relative to the date of maximum rainfall.

and sensible cooling (heating) of the ocean (atmosphere). Last but not least, the duration of the deep convective period is well correlated to the maximum MJO convective depth as indicated by minimum IR T_b (Figure 3e), suggesting deeper convection (colder cloud top) promotes longer deep convective period.

Four MJOs with long (cases 1–2) and short (cases 3–4) SDT periods (as marked in Figure 3) are examined further as an attempt to better identify specific processes during SDT (Figure 4). The SDT of MJOs 1–2 occurs gradually during a 2 week period, after a 5–10 day SCP (Figures 4a and 4b). The SCP of MJOs 1–2 feature a mode of convective cloud tops reaching only ~280 K (3–4 km asl), marking shallow cumulus. MJO 2 has a longer SCP (10 days) possibly due to drier conditions in the midtroposphere compared to MJO 1 (5 days). As mentioned earlier, the duration of SCP is negatively correlated with the relative humidity of the midtroposphere (Figure 3b). The SDT (red curves) of MJOs 1–2 occurs in the form of 2–3 pulses (3–4 days each) of active convection with cloud tops deepening from pulse to pulse. In the meantime, the midtrophosphere moistens (green curves) gradually with similar time scales as SDT, indicating positive feedbacks between midlevel moistening and convective deepening. Deep convection commences after the midtroposphere is significantly moist (RH at 500 hPa ~70%), consistent with results based on atmospheric soundings [*Ruppert and Johnson*, 2015]. SST (blue curves) increases during the SDT but maximizes prior to the onset of deep convection, especially for MJO 1 (SST of MJO 2 is possibly reduced by upper ocean mixing due to stronger winds).

The other two MJOs (Figures 4c and 4d) exhibit an extremely rapid SDT (2–3 days) after experiencing an extended SCP (~2 weeks). During the 2 week period of the SCP, the midtroposphere was dry (RH of 30–40%) and winds were calm (2–3 m s^{-1}), indicating a notable suppressed condition possibly associated with significant large-scale subsidence and lack of instability. However, SSTs continue to increase and achieved relatively high values (>30°C) during the suppressed period, as upper ocean mixing is reduced and a diurnally warmed layer of near surface water can develop during weak wind situations [*Matthews et al.*, 2014]. With such high SSTs, surface heat fluxes and low-level humidity are enhanced, further increasing atmospheric instability. In this case, the atmospheric instability keeps accumulating during the extended period of shallow convection. The release of instability accumulated during this time may then lead to a very short SDT period and rapid development of deep convection (as documented in these two cases). During these two MJOs, tropospheric moistening time periods are also shortened compared to the first two cases, possibly due to the dominance of moistening by large-scale mechanisms [*Hagos et al.*, 2014], a factor that was not quantified in our study.

4. Summary and Discussion

This study examines the convective evolution of 74 full MJO cycles over the central IO during 1998–2013. Various convective periods, especially the SDT, are identified by TRMM convective cloud tops (IR T_b). Our study was partially motivated by reported discrepancies in SDT between climatological-based composites using reanalysis data [*Benedict and Randall*, 2007] and new observational and modeling studies from DYNAMO [*Ruppert and Johnson*, 2015; *Powell and Houze*, 2015a, 2015b; *Hagos et al*., 2014]. Our study addresses the SDT time scale problem from a climatological observational perspective and case study basis and explores potential factors impacting SDT duration.

Our results show that SDT exhibits a broad spectrum of 2–20 days with median values of 8–10 days. Nearly 50% of the SDTs fall in the 10–20 day period, while ~25% are less than one week in duration. The gradual SDT processes (10–20 days) which is consistent with the discharge-recharge hypothesis [*Benedict and Randall*, 2007] occurs a factor of two more often compared to the short SDT period (<7 days) such as observed during DYNAMO [*Powell and Houze*, 2015a, 2015b]. This gradual convective deepening of the 10–20 day SDT is consistent with the gradual moistening in the troposphere based on long-term MJO composites [*Benedict and Randall*, 2007], suggesting positive feedbacks between convective deepening and tropospheric moistening. Short SDT durations are far from rare, indicating the important role of moistening by large-scale mechanisms such as uplift and horizontal moisture convergence. However, it cannot be ruled out that physical processes of discharge-recharge theory can work on time scales of rapid SDTs. Furthermore, this study cannot determine whether congestus moistening is secondary to moistening by large-scale mechanisms (e.g., uplift and moisture convergence) during rapid SDTs or whether large-scale mechanisms play a secondary role to local moistening in gradual SDTs. Future work will examine the relative importance of various moistening mechanisms (e.g., congestus moistening versus large-scale mechanisms) as a function of SDT time scale.

This study also finds that SDT time scale is negatively correlated to SCP duration. For example, extremely short (extended) SCPs are followed by gradual (rapid) SDTs prior to the onset of MJO deep convection. We speculate that SST, convective available potential energy and moisture are accumulated during extended suppressed periods thus leading to a sudden outbreak of deep convection. Perhaps shallow cumulus over an extended period can also sufficiently moisten and warm the lower troposphere, thereby shortening the SDT duration. In cases of short SCP, the environment may be favorable for the development of congestus, but not yet for deep convection, and therefore convective depth may only gradually grow through convective moistening. The weak relationship between SDT time scale and a single environmental parameter indicates that SDT is influenced simultaneously by multiple factors/processes, which is also the goal of our future analysis.

Matthews [2008] found that precursor signals proposed by previous studies are evident in "successive" MJOs (with preceding MJOs) but are absent in the "primary" MJOs (no preceding MJO), suggesting a different nature of convective initiation between primary and successive MJOs. In this study, we have identified primary MJO events sampled by TRMM using initiation dates from *Yong and Mao* [2015], which applied the same definition as *Matthews* [2008]. By this methodology, 10 (out of 12) primary MJOs were identified (with sufficient TRMM samples) during 1998–2010 (common time period between Yong and Mao study and ours). Histograms of the time scales of convective development of these 10 primary MJOs have been added to Figure 2 (green bars). Compared to the total MJO population, primary MJOs tend to have slightly longer SDT time scale (Figure 2b) but shorter SCP (Figure 2c) and deep convective periods (Figure 2d). These opposite tendencies of SDT and SCP time scales for primary MJOs are actually consistent with previously shown negative correlations between SDT and SCP durations (Figure 3a). Note that suppressed periods of primary MJOs are generally shorter and have reduced amplitudes compared to successive MJOs [*Matthews*, 2008]. Shorter SCP in primary MJOs could lead to longer SDT as discussed previously. As far as environmental conditions, primary MJOs generally have lower SSTs and weaker midtropospheric moistening prior to the MJO onset (not shown), consistent to the finding by *Matthews* [2008] that primary MJOs do not show any precursory signals (increasing trend) in SST and tropospheric moistening. As a result, primary MJOs tend to have weaker convective intensity thus a shorter duration for deep convection (Figure 2d). Due to the reduced samples (only 10–12) of primary MJOs during 1998–2013, it is not statistically robust to separate our data set into primary and successive MJOs and conduct detailed comparisons between these two groups. This problem certainly motivates a future study to fully investigate convective development (e.g., SDT) of primary versus successive MJOs using longer-term satellite and reanalysis data.

Acknowledgments
This research was supported by the National Science Foundation grant AGS-1063928 and the NASA PMM grant NNX13AG32G. We thank our colleagues for insightful discussions of this work, especially Elizabeth Thomson, James Benedict, David Randall and Richard Johnson from CSU, and Chidong Zhang (University of Miami). Special thanks go to the two anonymous reviewers for their positive and constructive suggestions. DYNAMO data are available from NCAR's data archive: http://data.eol.ucar.edu/master_list/?project=DYNAMO. The TRMM satellite data can be downloaded from NASA Goddard Earth Sciences Data and Information Services Center (http://disc.sci.gsfc.nasa.gov/TRMM). Satellite-based SST data are available from (http://www.remss.com/measurements/sea-surface-temperature).

References

Awaka, J., T. Iguchi, and K. Okamoto (2009), TRMM PR standard algorithm 2A23 and its performance on bright band detection, *J. Meteorol. Soc. Jpn.*, *87*, 31–52.
Bechtold, P., M. Köhler, T. Jung, F. Doblas-Reyes, M. Leutbecher, M. J. Rodwell, F. Vitart, and G. Balsamo (2008), Advances in simulating atmospheric variability with the ECMWF model: From synoptic to decadal time-scales, *Q. J. R. Meteorol. Soc.*, *134*, 1337–1351.
Benedict, J. J., and D. A. Randall (2007), Observed characteristics of the MJO relative to maximum rainfall, *J. Atmos. Sci.*, *64*, 2332–2354.
Bladé, I., and D. L. Hartmann (1993), Tropical intraseasonal oscillations in a simple nonlinear model, *J. Atmos. Sci.*, *50*, 2922–2939.
Dee, D. P., et al. (2011), The ERA-Interim reanalysis: Configuration and performance of the data assimilation system, *Q. J. R. Meteorol. Soc.*, *137*, 553–597.
Del Genio, A. D., Y. Chen, D. Kim, and M.-S. Yao (2012), The MJO transition from shallow to deep convection in CloudSat/CALIPSO and GISS GCM simulations, *J. Clim.*, *25*, 3755–3770.
Gentemann, C. L., T. Meissner, and F. J. Wentz (2010), Accuracy of satellite sea surface temperatures at 7 and 11 GHz, *IEEE Trans. Geosci. Remote Sens.*, *48*, 1009–1018.
Hagos, S., Z. Feng, K. Landu, and C. N. Long (2014), Advection, moistening, and shallow-to-deep convection transitions during the initiation and propagation of Madden-Julian Oscillation, *J. Adv. Model. Earth Syst.*, *6*, 938–949, doi:10.1002/2014MS000335.
Hohenegger, C., and B. Stevens (2013), Preconditioning deep convection with cumulus congestus, *J. Atmos. Sci.*, *70*, 448–464.
Hu, Q., and D. A. Randall (1994), Low-frequency oscillations in radiative-convective systems, *J. Atmos. Sci.*, *51*, 1089–1099.
Huffman, G. J., D. T. Bolvin, E. J. Nelkin, D. B. Wolff, R. F. Adler, G. Gu, Y. Hong, K. P. Bowman, and E. F. Stocker (2007), The TRMM multisatellite precipitation analysis (TMPA): Quasi-global, multiyear, combined-sensor precipitation estimates at fine scales, *J. Hydrometeorol.*, *8*, 55–38.
Hung, M.-P., J.-L. Lin, W. Wang, D. Kim, T. Shinoda, and S. J. Weaver (2013), MJO and convectively coupled equatorial waves simulated by CMIP5 climate models, *J. Clim.*, *26*, 6185–6214.
Johnson, R. H., T. M. Rickenbach, S. A. Rutledge, P. E. Ciesielski, and W. H. Schubert (1999), Trimodal characteristics of tropical convection, *J. Atmos. Sci.*, *58*, 2729–2750.
Kemball-Cook, S. R., and B. C. Weare (2001), The onset of convection in the Madden-Julian oscillation, *J. Clim.*, *14*, 780–793.
Kikuchi, K., and Y. N. Takayabu (2004), The development of organized convection associated with the MJO during TOGA COARE IOP: Trimodal characteristics, *Geophys. Res. Lett.*, *31*, L10101, doi:10.1029/2004GL019601.
Kim, D., et al. (2009), Application of MJO simulation diagnostics to climate models, *J. Clim.*, *22*, 6413–6436.
Kummerow, C., W. Barnes, T. Kozu, J. Shiue, and J. Simpson (1998), The tropical rainfall measuring mission (TRMM) sensor package, *J. Atmos. Oceanic Technol.*, *15*, 809–817.
Lafleur, D. M., B. S. Barrett, and G. R. Henderson (2015), Some climatological aspects of the Madden–Julian Oscillation (MJO), *J. Clim.*, *28*, 6039–6053.
Lin, J.-L., et al. (2006), Tropical intraseasonal variability in 14 IPCC AR4 climate models. Part I: Convective signals, *J. Clim.*, *19*, 2665–2690.
Madden, R. A., and P. R. Julian (1971), Detection of a 40-50-day oscillation in the zonal wind in the tropical Pacific, *J. Atmos. Sci.*, *28*, 702–708.
Madden, R. A., and P. R. Julian (1972), Description of global-scale circulation cells in the tropics with a 40-50 day period, *J. Atmos. Sci.*, *29*, 1109–1123.
Masunaga, H. (2013), A satellite study of tropical moist convection and environmental variability: A moisture and thermal budget analysis, *J. Atmos. Sci.*, *70*, 2443–2466.
Matthews, A. J. (2008), Primary and successive events in the Madden-Julian oscillation, *Q. J. R. Meteorol. Soc.*, *134*, 439–453.
Matthews, A. J., D. B. Baranowski, K. J. Heywood, P. J. Flatau, and S. Schmidtko (2014), The surface diurnal warm layer in the Indian Ocean during CINDY/DYNAMO, *J. Clim.*, *27*, 9101–9122.
Powell, S. W., and R. A. Houze Jr. (2013), The cloud population and onset of the Madden-Julian Oscillation over the Indian Ocean during DYNAMO-AMIE, *J. Geophys. Res. Atmos.*, *118*, 11,979–11,995, doi:10.1002/2013JD020421.
Powell, S. W., and R. A. Houze Jr. (2015a), Evolution of precipitation and convective echo top heights observed by TRMM radar over the Indian Ocean during DYNAMO, *J. Geophys. Res. Atmos.*, *120*, 3906–3919, doi:10.1002/2014JD022934.
Powell, S. W., and R. A. Houze Jr. (2015b), Effect of dry large-scale vertical motions on initial MJO convective onset, *J. Geophys. Res. Atmos.*, *120*, 4783–4805, doi:10.1002/2014JD022961.
Riley, E. M., B. E. Mapes, and S. N. Tulich (2011), Clouds associated with the Madden-Julian oscillation: A new perspective from CloudSat, *J. Atmos. Sci.*, *68*, 3032–3051.
Ruppert, J. H., Jr., and R. H. Johnson (2015), Diurnally modulated cumulus moistening in the preonset stage of the Madden–Julian Oscillation during DYNAMO, *J. Atmos. Sci.*, *72*, 1622–1647.
Stephens, G. L., P. J. Webster, R. H. Johnson, R. Engelen, and T. S. L'Ecuyer (2004), Observational evidence for the mutual regulation of the tropical hydrological cycle and the tropical sea surface temperatures, *J. Clim.*, *17*, 2213–2224.
Virts, K. S., and J. M. Wallace (2010), Annual, interannual, and intraseasonal variability of tropical tropopause transition layer cirrus, *J. Atmos. Sci.*, *67*, 3097–3112.
Vitart, F., and F. Molteni (2010), Simulation of the Madden–Julian oscillation and its teleconnections in the ECMWF forecast system, *Q. J. R. Meteorol. Soc.*, *136*, 842–855.
Wheeler, M., and H. H. Hendon (2004), An all-season real-time multivariate MJO index: Development of an index for monitoring and prediction, *Mon. Weather Rev.*, *132*, 1917–1932.
Xu, W., and S. A. Rutledge (2014), Convective characteristics of the Madden-Julian Oscillation over the central Indian Ocean observed by shipborne radar during DYNAMO, *J. Atmos. Sci.*, *71*, 2859–2877.
Xu, W., S. A. Rutledge, C. Schumacher, and M. Katsumata (2015), Evolution, properties, and spatial variability of MJO convection near and off the Equator during DYNAMO, *J. Atmos. Sci.*, *72*, 4126–4147.
Yoneyama, K., C. Zhang, and C. N. Long (2013), Tracking pulses of the Madden-Julian Oscillation, *Bull. Am. Meteorol. Soc.*, *94*, 1871–1891.
Yong, Y., and J. Mao (2015), Mechanistic analysis of the suppressed convective anomaly precursor associated with the initiation of primary MJO events over the tropical Indian Ocean, *Clim. Dyn.*, *46*, 779–795.
Zhang, C. (2005), Madden-Julian oscillation, *Rev. Geophys.*, *43*, RG2003, doi:10.1029/2004RG000158.
Zhang, C. (2013), Madden-Julian oscillation: Bridging weather and climate, *Bull. Am. Meteorol. Soc.*, *94*, 1849–1870.
Zhang, G. J., and X. Song (2009), Interaction of deep and shallow convection is key to Madden-Julian Oscillation simulation, *Geophys. Res. Lett.*, *36*, L09708, doi:10.1029/2009GL037340.